

# Ground-Based Radiometric Profiling during Dynamic Weather Conditions

R. Ware<sup>1,2</sup>, P. Herzegh<sup>3</sup>, F. Vandenberghe<sup>3</sup>, J. Vivekanandan<sup>3</sup>, and E. Westwater<sup>4</sup>

<sup>1</sup>Corresponding Author: Radiometrics Corporation, 2840 Wilderness Place  
Boulder, CO 80301-5414, 303 449-9192, [ware@radiometrics.com](mailto:ware@radiometrics.com)

<sup>2</sup>University Corporation for Atmospheric Research, Boulder, CO 80307

<sup>3</sup>National Center for Atmospheric Research, Boulder, CO 80307

<sup>4</sup>Cooperative Institute for Research in the Environmental Sciences, University of Colorado/  
NOAA Environmental Technology Laboratory, Boulder, CO 80305

*Submitted to the Journal of Applied Meteorology  
26 December 2003*

## Capsule

We discuss radiometric profiling during dynamic weather conditions and show that the accuracy of radiometric retrievals is similar to radiosonde soundings when used for numerical weather prediction. We present example thermodynamic profile retrievals during weather conditions including fog, snow, summer monsoon, and boundary layer turbulence.

## Abstract

Continuous temperature and humidity soundings up to 10 km height and one-layer cloud liquid soundings can be retrieved from ground-based multi-channel microwave radiometer observations. We show that the accuracy of thermodynamic retrievals from the radiometric observations is similar to radiosonde soundings when used for numerical weather prediction. We present example thermodynamic retrievals during a variety of dynamic weather conditions including fog, snowfall, summer monsoon, and boundary layer turbulence. We discuss results from other studies that combine slant delay observations from GPS networks with thermodynamic soundings to provide high resolution three dimensional water vapor analysis. The preliminary results presented suggest that radiometric methods for continuous thermodynamic profiling have significant potential for a variety of applications in meteorological research and weather forecasting.

## Introduction

The thermodynamic state of the atmosphere is traditionally probed twice daily by radiosondes at multiple locations on land to provide vertical profile information needed for weather prediction. However, twice-per-day soundings fail to track the changes in thermodynamic structure that occur on temporal scales of minutes to hours. These changes are often crucial to accurate weather prediction and are inadequately resolved by satellite measurements, particularly during cloudy conditions and in the terrestrial boundary layer. Continuous thermodynamic monitoring by ground-based radiometric profilers can be used to fill the temporal gaps between radiosonde soundings. A general description of ground-

based atmospheric profiling with microwave radiometry is provided by Westwater [1993], and experimental results from a 6-channel radiometer are discussed by Hogg et al. [1983].

We present thermodynamic retrievals from a commercial radiometric profiler<sup>1</sup> during dynamic weather conditions. The radiometer observes atmospheric brightness temperatures in 5 frequency bands from 22 to 30 GHz, and in 7 bands from 51 to 59 GHz [Solheim et al., 1998]. It also measures zenith infrared temperature, and surface temperature, humidity and pressure. The radiometer has automated elevation and azimuth scanning capability, and the observation interval can be as short as several seconds. The instrument is portable, with 0.12 m<sup>3</sup> volume and 32 kg weight. Historical radiosonde and neural network or regression methods are used for profile retrieval. Retrievals include temperature and humidity soundings up to 10 km height, and one-layer cloud liquid soundings.

Radiometric retrievals are similar in accuracy to radiosonde soundings when used for numerical weather prediction [Ware et al., 2003a]. Radiosonde assimilation errors used by the National Centers for Environmental Prediction for numerical weather analysis<sup>2</sup>, and radiometric retrieval error determined from statistical comparisons with radiosondes [Güldner and Spänkuch, 2001; Liljegren, 2001] are shown in Figure 1. Retrieval error is smaller than radiosonde sounding error for boundary layer temperatures, and slightly higher above the boundary layer. Retrieval error is smaller than radiosonde sounding error for water vapor at all heights. The dominant radiosonde error is *representativeness* error resulting from characterization of a model cell volume by a point measurement. Radiometric retrievals are based on volumetric measurements<sup>3</sup> and are less susceptible to representativeness error than radiosonde soundings.

We discuss examples of radiometric retrievals at Boulder, Colorado, and comparisons with Denver radiosonde soundings during dynamic weather conditions including fog, summer monsoon, snowfall, and boundary layer turbulence. For these examples the radiometer measurements were made at 5 minute intervals, and retrievals were obtained using neural network methods. We also describe results from other studies demonstrating the potential for improved numerical weather prediction using slant delay observations from GPS networks combined with radiometric profiler observations.

### **Upslope with Supercooled Fog**

Upslope weather conditions occurred in the Denver area east of the Colorado Front Range during 16 to 21 February 2001. Radiometric retrievals up to 2 km height at Boulder on 16 Feb 01 are shown in Figure 2. The arrival of cold upslope air near 1100 UTC on 16 Feb 01 is seen in the radiometric temperature retrievals (upper contour) below 500 m height, accompanied by sharp increases in relative humidity (middle contour) and cloud liquid water (lower contour). Cloud liquid reached a maximum density of 0.32 g/m<sup>3</sup> at 300 m height at 1716 UTC. Cloud base height, which is automatically retrieved from infrared measurements of cloud base temperature (left column, bottom plot) and the retrieved temperature profile, is indicated in the upper contour plot. The temperature profile shows that the fog is supercooled, with a minimum temperature of -11 C. A 10 C decrease in surface temperature (left column, first plot), a 45% increase in surface relative humidity (left column, second plot), and a 10 mb increase in surface pressure (left column, third plot) occurred from 0000 to 1200 UTC. Sudden onset of fog is indicated by sharp increases in zenith infrared temperature (left column, bottom plot); and integrated liquid (bottom row, fourth plot), which increases to a maximum of 0.19 mm at 1716 UTC. The integrated vapor retrieval (bottom row, third plot) shows a gradual decrease from 0.58 cm at 0000

---

<sup>1</sup>The TP/WVP-3000 is manufactured by Radiometrics Corporation <<http://radiometrics.com>>.

<sup>2</sup><http://lnx21.wwb.noaa.gov/oberr/reanl-obs.html>.

<sup>3</sup>The antenna beamwidth of the radiometric profiler ranges from 2 to 6 degrees.

UTC to 0.49 cm at 1120 UTC, followed by a gradual increase to 0.63 cm at 2204 UTC. The radiometer rain sensor (bottom row, second plot) shows no moisture accumulation.

A comparison of the radiometer retrieval at Boulder and the 1200 UTC 16 Feb 2001 radiosonde sounding at Denver (located 50 km southeast of Boulder) is shown in Figure 3. A temperature inversion at 1 km height, near saturation of relative humidity below 500 m height, and tropopause height below 10 km are seen in both the radiometric retrieval and radiosonde sounding. Fog with a maximum density of  $0.14 \text{ g/m}^3$  at 300 m height is seen in the retrieval.

Poor visibility and icing conditions during this upslope event led to major disruptions in surface and air transportation in the Denver area, including diversion of flights from Denver International Airport for 18 hours. Fog was not predicted by numerical forecasts that used the Denver rawinsonde. However, variational assimilation of Boulder radiometric retrievals led to accurate fog forecasts in the Boulder-Denver area [Vandenberghe and Ware, 2003].

Both the 0000 UTC 16 Feb 01 Boulder radiometric retrieval (Figure 3) and Denver radiosonde sounding (not shown) showed 45% or less relative humidity below 500 m height. During the following 12 hours, the 5-min radiometric relative humidity retrievals steadily increased to greater than 90%, with the first fog retrieval occurring at 1141 UTC. A similar trend was observed in Boulder prior to supercooled fog, freezing drizzle, and snow that occurred on 4 March 2003. Radiometric retrievals, weather radar, cloud radar, lidar and tower observations during this weather event are discussed by Herzegh et al. [2003] and by Rasmussen and Ikeda [2003]. This suggests that trends of continuous relative humidity retrievals can be used to predict the onset of fog. Increased skill is expected if raw radiometric brightness temperatures instead of retrieved radiometric profiles are assimilated into numerical weather models [Nehrkorn et al., 2003].

Radiometric profiler, weather and cloud radar, lidar, and tower observations during a similar Colorado upslope storm including supercooled fog, freezing drizzle, and snow are described by Herzegh et al. [2003], and by Rasmussen and Ikeda, [2003].

## **Snowfall**

Radiometric retrievals during a snowfall event in Boulder, Colorado, on 23 December 2003 are shown in Figure 4. Relatively dry snow that sublimated several minutes after touching the ground were visually observed at the radiometer site. Temperature profiles up to 3 km height (upper contour) are below freezing, showing gradual 4 C heating below 500 m height from 1600 to 2100 UTC followed by gradual 2 C cooling. Relative humidity ranges from 90 to 100% from 0.5 to 2 km height during most of the observation period (middle contour). “Equivalent” liquid density variations with ~15 min period and  $0.1 \text{ g/m}^3$  magnitude are seen from 500 m to 1.2 km height from 2050 to 2210 UTC (bottom contour plot). The liquid density retrieval is termed “equivalent” because the physical retrieval model is based on liquid emission only and does not include ice and scattering. If ice and scattering are included in the retrieval model, liquid and ice retrievals can be obtained [Li et al., 1997].

The Denver radiosonde sounding at 0000 UTC on 24 Dec 02 and the Boulder radiometer retrieval at 2354 UTC on 23 Dec 02 are shown in Figure 5. Both soundings show similar temperature lapse rates and tropopause height below 10 km. The radiometric temperature retrieval is ~2 to 3 K warmer than the radiosonde sounding from 1 to 3 km height, and is ~8 K warmer at the tropopause. The radiosonde relative humidity measurement increases from 65% at the surface to 80% at 700 m height and then remains above 75% up to 4.5 km height. The retrieved relative humidity increases from 80% at the surface to saturation at 900 m and remains saturated to 1.75 km. We attribute the temperature and relative humidity disagreements in Figure 5 to differences between point (radiosonde) and volume

(radiometer) measurements, their vertical resolution characteristics, and to atmospheric variability over the 50 km distance between the two measurements.

During the 11 hours prior to snowfall, relative humidity at 1 km height steadily increased from 50% to 100%. Since saturation is required for cloud and precipitation formation, relative humidity profile trends could potentially improve local short term cloud and precipitation forecasting.

### **Summer Monsoon**

High levels of relative humidity (middle contour) and intermittent cloud at 3 to 5 km height (bottom contour) associated with summer monsoon conditions on 19 to 20 August 2002 at Boulder are shown in Figure 7. Surface temperature (left column, upper plot) shows a general solar heating trend from 2130 to 2250 UTC, cooling under cloudy skies (cloud base height is shown in the upper contour) from 2300 to 2350 UTC, solar heating under clear skies from 0000 to 0020 UTC on 20 Aug, and steady cooling thereafter as the sun descends. The rain flag (bottom row, second panel) indicates a rain shower at 2355 UTC on 19 Aug, with the integrated water vapor reaching a 1.8 cm minimum at 2220 UTC and then steadily increasing to a 2.59 cm maximum at 0110 UTC on 20 Aug. The integrated liquid water (bottom row, third panel) is highly variable, reaching a sharp 0.26 mm maximum at 2310 UTC on 19 Aug.

The Denver radiosonde sounding at 0000 UTC 20 Aug 2002 and the Boulder radiometer retrieval 52 minutes earlier at 2308 UTC (the time that the integrated liquid reaches a 0.2 mm maximum) are shown in Figure 8. Both soundings show similar temperature lapse rates. However, the retrieved temperature profile at Boulder is  $\sim 2$  K higher than the Denver radiosonde sounding from 1 to 2 km height, and is  $\sim 2$  to 4 K higher from 5 to 10 km. Both relative humidity measurements steadily increase from 20% at the surface with the radiometer retrieval reaching a maximum of 85% just above 4 km height and the radiosonde sounding reaching several maxima around 90% from just below 4 km to just above 6 km height. The retrieved cloud liquid profile extends from 3 to 5 km height and reaches a maximum density of  $0.18 \text{ g/m}^3$ . Continuous relative humidity and cloud liquid soundings can potentially be used to improve short term precipitation forecasts. The importance of the initial relative humidity field in numerical rainfall prediction is discussed by Ducroqc et al. [2003].

### **Boundary Layer Turbulence**

Strong gusty winds were reported in the foothills to the west of Boulder on 12 December 2002. Retrievals to 1 km height from radiometric profiler observations (Figure 8) show boundary layer temperature fluctuations as large as 3 C (upper contour plot) from 1130 to 1530 UTC on this day. Surface pressure variations (left column, third panel) as large as 0.6 mb were also observed that are out of phase with the temperature variations. The average period of the variations is 13 minutes. Similar variations were seen in retrievals from two additional radiometric profilers at the same location. Relatively clear skies prevailed during the observation period, as indicated by the cloud base temperature (left column, lower panel) and integrated liquid water (bottom row, fourth panel) time series. The boundary layer thermodynamic variations are consistent with the presence of boundary layer gravity waves.

The Denver radiosonde sounding at 1200 UTC on 20 December 2002 and the Boulder radiometer retrieval at 1154 UTC are shown in Figure 9. Both soundings show an 8 C nocturnal boundary layer temperature inversion. The inversion height is 200 m for the radiosonde sounding at Denver and 400 m for the radiometric retrieval at Boulder. Vertical resolution can be significantly improved with retrievals based on radiometric observations at multiple elevation angles [Westwater et al., 2000]. The two soundings are similar from 2 to 7 km with a maximum difference of 2 C between 3 and 4 km height. Both soundings show the tropopause height below 10 km, which typically occurs when the jet stream is south of the sounding location and is associated with unstable weather conditions. The maximum

difference in the two soundings occurs at the tropopause, where the radiosonde measurement is 7 C colder than the retrieval. The relative humidity profiles are similar with surface measurements of 45% at Denver and 60% at Boulder, and relatively dry conditions at all heights. Differences in the two relative humidity measurements can be attributed to atmospheric variability over the 50 km distance between the two observation sites, to differences in point and volumetric measurement methods, and to 25% peak to peak uncertainty in radiosonde humidity measurements [Turner et al., 2003].

### **Potential for Radiometric Profiling Combined with Slant GPS**

Radiometric profiling provides strong constraints on local water vapor fields. These local constraints can be extended to regional scales by combining local radiometric observations with slant observations from ground-based GPS networks. Slant GPS observations provide strong horizontal constraints on water vapor fields. By combining radiometric profiling and slant GPS observations, high resolution three dimensional water vapor analysis can be obtained. Combined radiometric observations and slant observations from a GPS network and their meteorological potential are described by MacDonald et al. [2002] and by Ware et al. [2003]. Significant improvements in convective storm and dispersion forecasting are expected.

### **Discussion**

Radiometric profiling provides temperature and humidity soundings with accuracy equivalent to radiosondes when used for numerical weather modeling, as well as single layer cloud liquid soundings. Case studies of radiometric retrievals were presented during upslope conditions including supercooled fog, and during snowfall, summer monsoon, and boundary layer turbulence. The case studies show that radiometric profiling provides new insights into short term thermodynamics of the atmosphere. Retrieved profiles can be assimilated into numerical weather models providing continuous thermodynamic constraints with the potential to improve short term forecasting. This potential is expected to increase if the observed radiometric brightness temperatures are directly assimilated into numerical weather models. Radiometric profiling can be combined with slant observations from GPS networks to obtain high accuracy three dimensional water vapor analysis. The preliminary results presented suggest that radiometric methods for continuous thermodynamic profiling have significant potential for a variety of applications in meteorological research and weather forecasting.

### **Acknowledgements**

Support from U.S. Army Research Laboratory contract DAAD17-01-C-0045 (E. Measure, Program Manager) is gratefully acknowledged.

### **References**

- Ducroqc, V., D. Ricard, J.-P. Lafore, and F. Orain, 2000: Storm-Scale Numerical Rainfall Prediction for Five Precipitating Events over France: On the Importance of the Initial Humidity Field, *Weather and Forecasting*, **17**, 1236-1256.
- Güldner, J., and D. Spänkuch, 2001: Remote sensing of the thermodynamic state of the atmospheric boundary layer by ground-based microwave radiometry, *J. Atmos. Ocean. Tech.*, **18**, 925-933.
- Herzogh, P., S. Landolt, and T. Schneider, 2003: The Structure, Evolution and Cloud Processes of a Colorado Upslope Storm as Shown by Profiling Radiometer, Radar, and Tower Data, *Proc. 31<sup>st</sup> Conf. on Radar Meteor.*, Seattle, WA, Amer. Met. Soc.
- Hogg, D., M. Decker, F. Guiraud, K. Earnshaw, D. Merritt, K. Moran, W. Sweezy, R. Strauch, E. Westwater, and G. Little, 1983: An Automatic Profiler of the Temperature, Wind and Humidity in the Troposphere, *J. Clim. Appl. Meteorol.*, **22**, 807-831.

- Li, L., J. Vivekanandan, C. H. Chan, and L. Tsang, 1997: Microwave radiometric technique to retrieve vapor, liquid and ice, *IEEE Trans. Geosci. Rem. Sens.*, **35**, 224-236.
- Liljegren, J., E. Clothiaux, S. Kato, B. Lesht, F., 2001: Initial Evaluation of Profiles of Temperature, Water Vapor and Cloud Liquid Water from a New Microwave Profiling Radiometer, *Proc. 5th Symp. Integrated Observing Systems*, Albuquerque, NM, Am. Met. Soc.
- MacDonald, A., Y. Xie, and R. Ware, 2002: Diagnosis of Three Dimensional Water Vapor Using Slant Observations from a GPS Network, *Mon. Wea. Rev.*, **130**, 386-397.
- Nehrkorn, T., and C. Grassotti, Mesoscale Variational Assimilation of Profiling Radiometer Data, *16<sup>th</sup> Conf. on Numerical Weather Prediction*, Seattle, WA, Amer. Met. Soc.
- Rasmussen, R., and K. Ikeda, 2003: Radar Observations of a Freezing Drizzle Case in Colorado, *31<sup>st</sup> Conf. on Radar Meteor.*, Seattle, WA, Amer. Met. Soc.
- Solheim, F., J. Godwin, E. Westwater, Y. Han, S. Keihm, K. Marsh, R. Ware, 1998: Radiometric Profiling of Temperature, Water Vapor, and Liquid Water using Various Inversion Methods, *Rad. Sci.*, **33**, 393-404.
- Turner, D., B. Lesht, A. Clough, J. Liljegren, H. Revercomb and D. Tobin, 2003: Dry Bias and Variability in Vaisala RS80-H Radiosondes: The ARM Experience, *J. Atm. Ocean. Tech.*, **20**, 117-132.
- Vandenberghe, F., and R. Ware, 2003: 4-Dimensional Variational Assimilation of Ground-Based Microwave Observations During a Winter Fog Event, *International Workshop on GPS Meteorology*, Tsukuba, Japan.
- Ware, R., R. Carpenter, J. Güldner, J. Liljegren, T. Nehrkorn, F. Solheim, and F. Vandenberghe, 2003a: A multi-channel radiometric profiler of temperature, humidity and cloud liquid, *Rad. Sci.*, **38**, 8079-8032.
- Ware, R., J. Braun, S.-Y. Ha, D. Hunt, Y.-H. Kuo, C. Rocken, M. Sleziak, T. Van Hove, J. Weber, R. Anthes, 2003b: Real-Time Water Vapor Sensing with SuomiNet – Today and Tomorrow, *Bull. Am. Met. Soc.* (submitted).
- Westwater, E., Ground-based Microwave Remote Sensing of Meteorological Variables, 1993: Chapter 4 in *Atmospheric Remote Sensing by Microwave Radiometry*, J. Wiley & Sons, Inc., M. Janssen (ed.), 145-213.
- Westwater, E., Y. Han, and F. Solheim, 2000: Resolution and Accuracy of a Multi-frequency Scanning Radiometer for Temperature Profiling, *Microw. Radiomet. Remote Sens. Earth's Surf. Atmosphere*, Pampaloni and Paloscia (ed.), VSP (publisher), The Netherlands, 129-135.

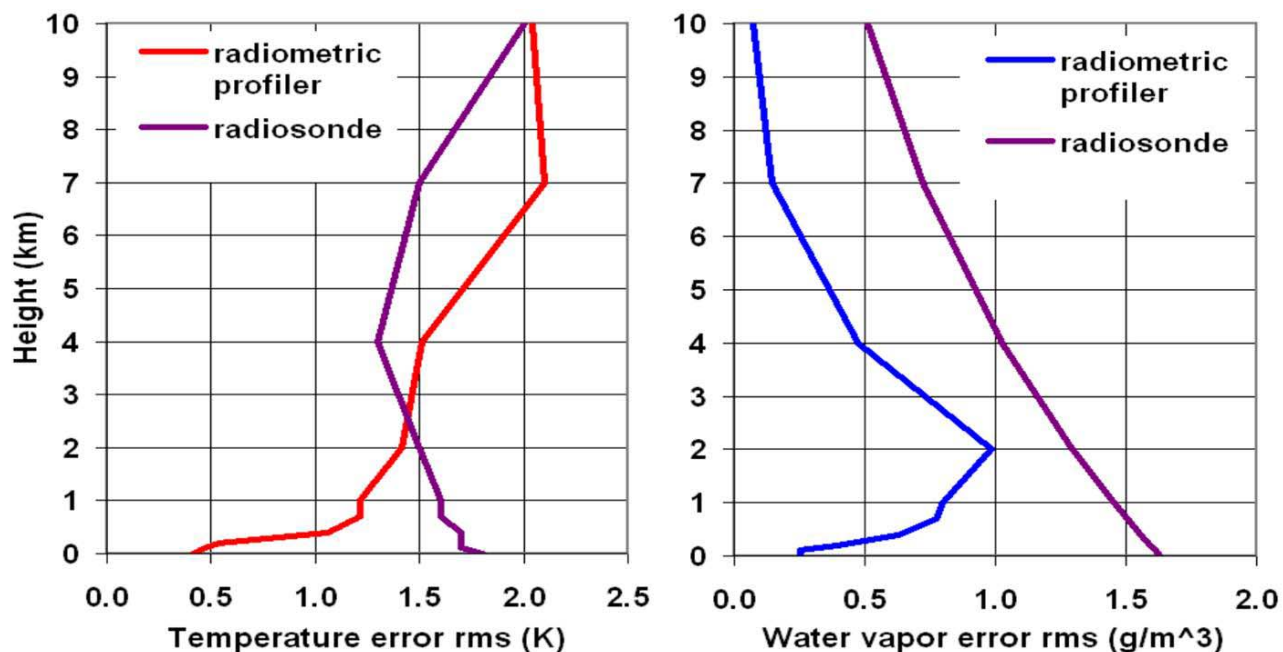


Figure 1. Radiometric retrieval accuracy determined by comparison with radiosondes. Radiosonde errors are provided by the National Centers for Environmental Prediction <<http://lnx21.wwb.noaa.gov/oberr/reanl-obs.html>>. Statistics of radiometric retrieval comparisons with radiosonde soundings are provided by Güldner and Spänkuch [2001] and by Liljegren, [2001].

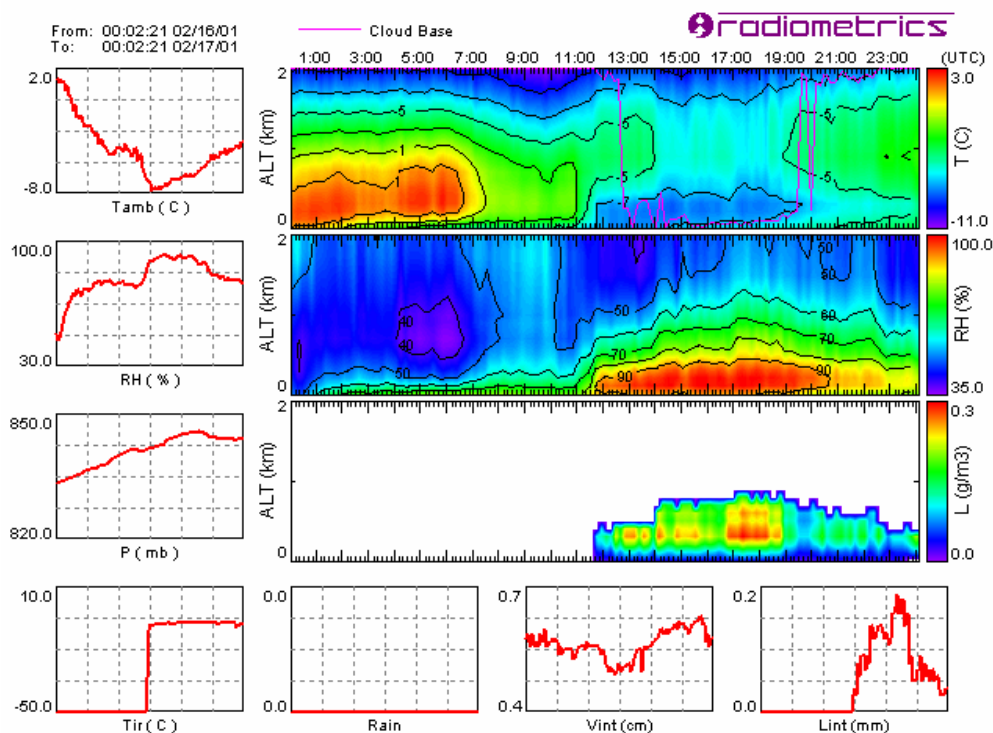


Figure 2. Radiometric retrievals to 2 km height showing supercooled fog associated with upslope weather conditions at Boulder on 16 Feb 01. Poor visibility and icing conditions during this upslope event led to major transportation disruptions including diversion of international flights from Denver

for 18 hours. Time series of temperature (upper contour), humidity (middle contour), and cloud liquid density (lower contour) profiles are shown along with surface temperature (left row, top plot), humidity (left row, second plot), and pressure (left row, third plot); zenith infrared temperature (left column, bottom plot); rain flag (lower row, second plot); and integrated water vapor (lower row, third plot) and integrated liquid water retrievals (lower row, fourth plot)<sup>4</sup>.

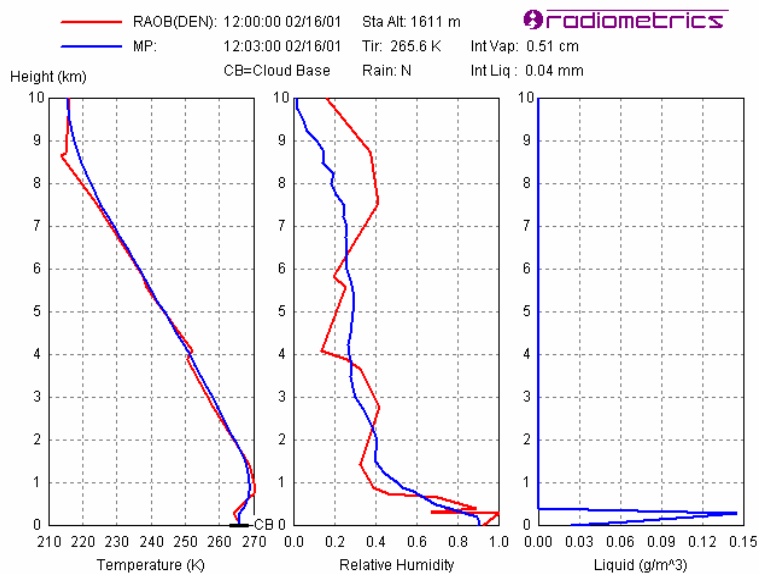


Figure 3. Boulder retrieval (blue) and Denver radiosonde sounding (red) showing supercooled fog, an inversion at 1 km height and relative humidity saturation up to 300 m height at 1200 UTC on 16 Feb 01. The radiometric retrieval shows 0.04 mm integrated liquid water and 0.14 g/m<sup>3</sup> maximum liquid water density<sup>5</sup>.

<sup>4</sup>Thermodynamic contours and other time series from radiometer measurements are displayed by VizMet<sup>R</sup> software developed by Radiometrics Corporation.

<sup>5</sup>Radiosonde and radiometric soundings are displayed by VizMet<sup>R</sup> software.

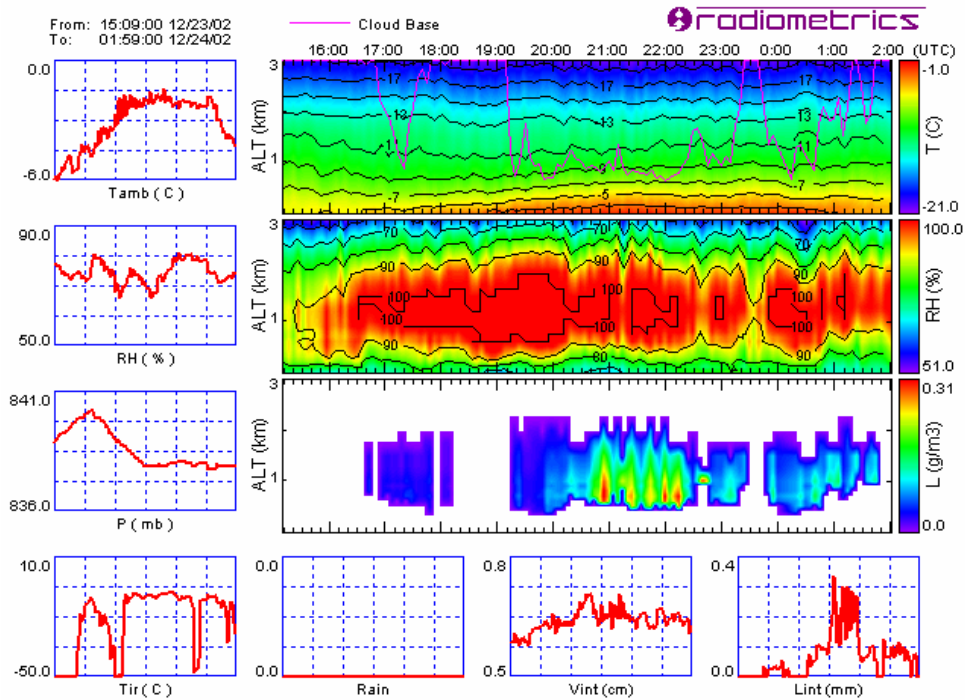


Figure 4. Radiometric retrievals to 3 km height during snowfall showing relative humidity saturation near 1 km height and waves of “equivalent” liquid at 15 min intervals on 23 Dec 02 at Boulder. Equivalent integrated liquid and liquid density maxima of 0.33 mm and 0.31 g/m<sup>3</sup> respectively are seen just before 2100 UTC.

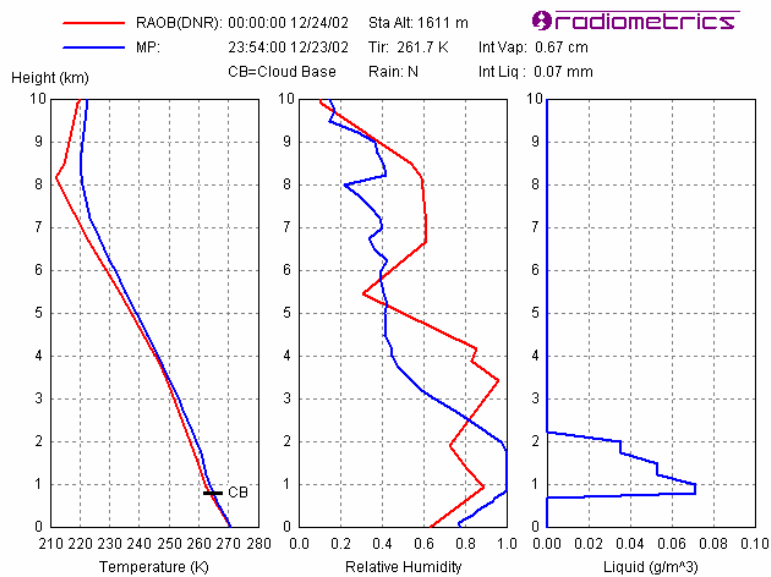


Figure 5. Boulder retrieval (blue) and Denver radiosonde (red) during snowfall at Boulder on 23 Dec 02. The retrieval shows relative humidity saturation from 1 to 2 km height and 0.07 g/m<sup>3</sup> equivalent liquid density near 1 km height. Tropopause height is seen in the radiosonde sounding and retrieval at 8.2 and 8.6 km height, respectively.

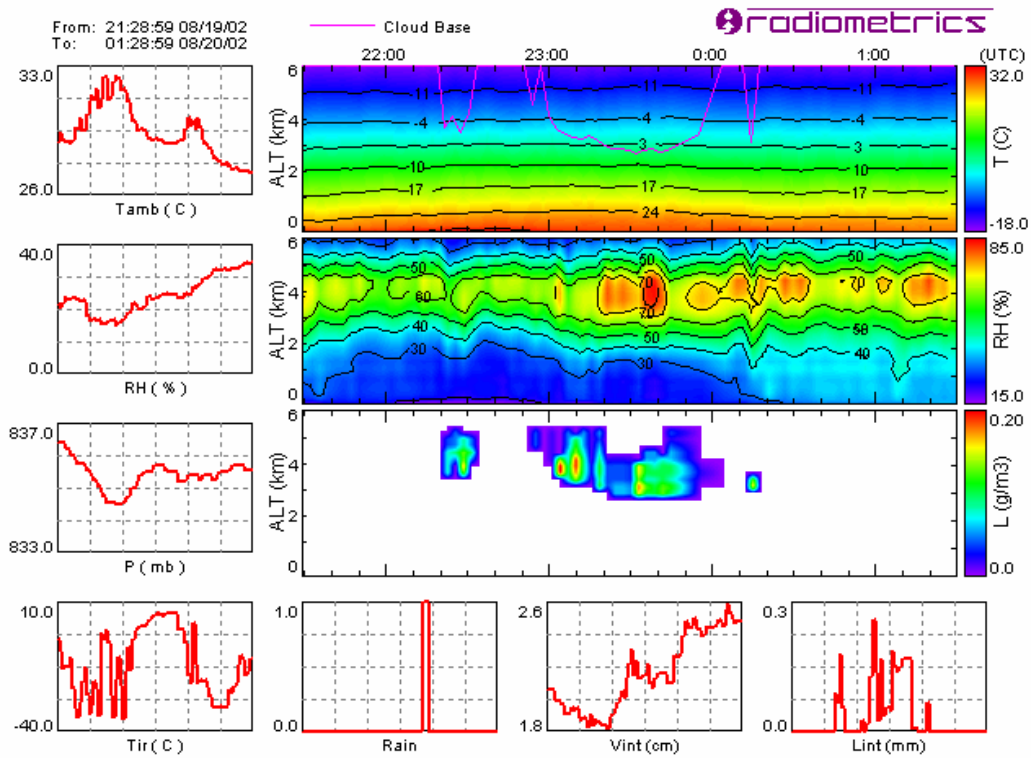


Figure 6. Radiometric retrievals to 6 km height during summer monsoon conditions showing elevated relative humidity and cloud liquid near 4 km height at Boulder on 19-20 Aug 02. The rain flag (bottom row, second plot) shows a brief rain shower.

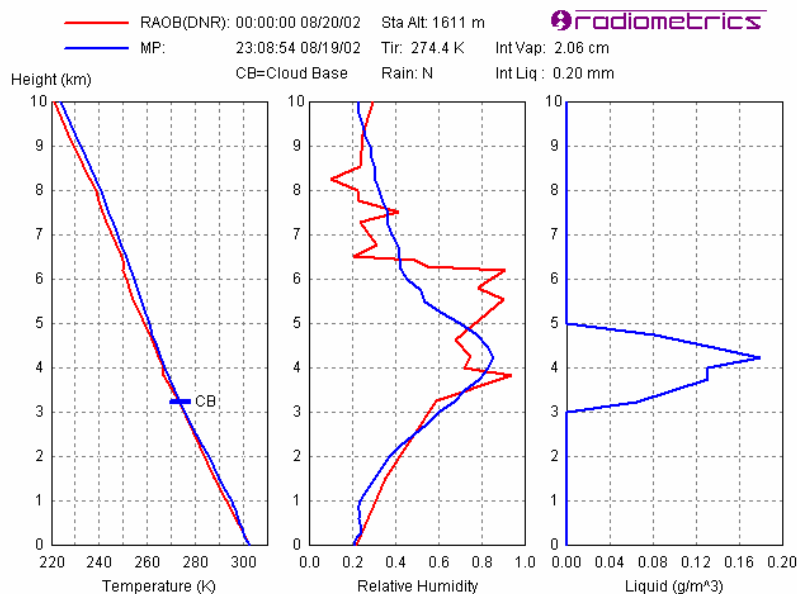


Figure 7. Boulder retrieval (blue) at 2308 UTC on 19 Aug 02 and Denver radiosonde sounding (red) at 0000 UTC on 20 Aug 02. Summer monsoon conditions show elevated humidity and liquid density near 4 km height and tropopause height above 10 km. The retrieval time was chosen to show the maximum liquid density ( $0.18 \text{ g/m}^3$ ) within one hour of the radiosonde launch time.

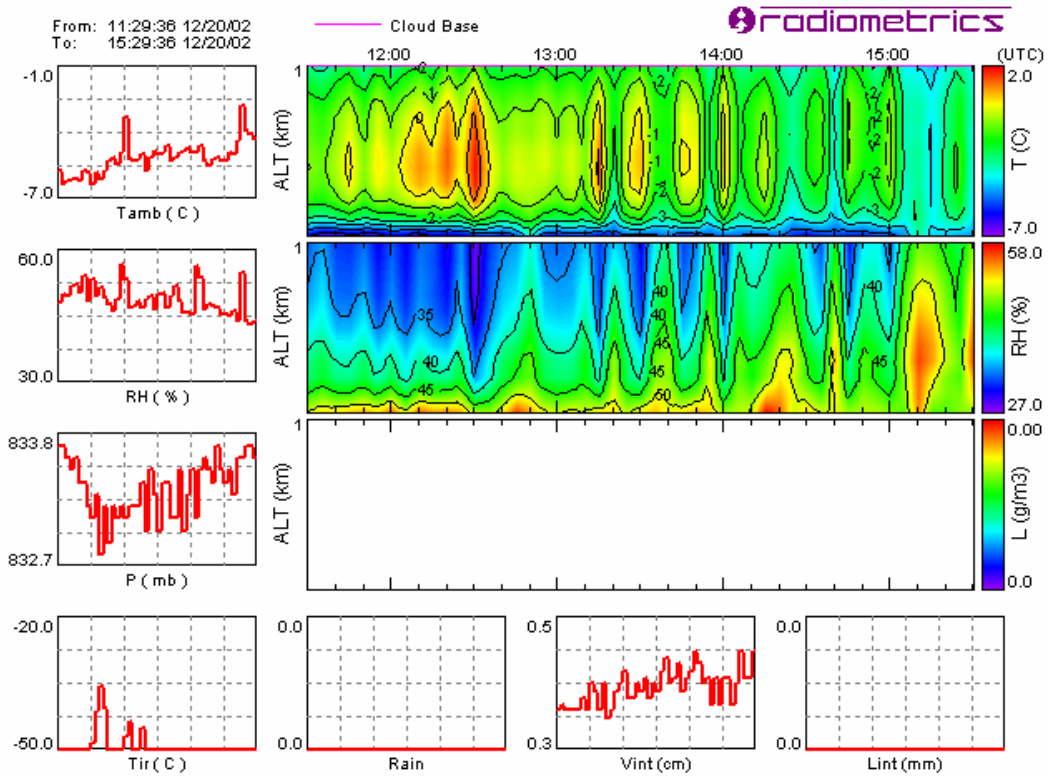


Figure 8. Radiometric retrievals to 1 km height showing 13-min periodic temperature variations associated with gusty winds and boundary layer turbulence at Boulder on 20 Dec 02. A strong temperature inversion is seen below 200 m height.

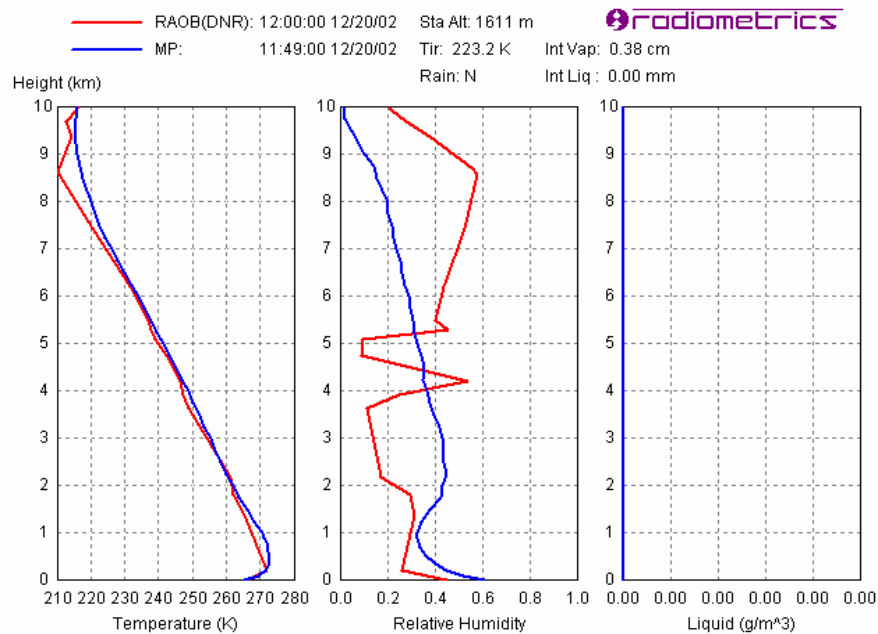


Figure 9. Boulder retrieval (blue) and Denver radiosonde sounding (red) showing strong surface temperature inversions and tropopause height below 10 km at Boulder on 20 Dec 03. The inversion height is 400 m in the radiometric retrieval and 200 m in the radiosonde sounding. Tropopause height below 10 km height and relative humidity less than 60% is seen in both plots.